DOI:
10.1109/TRO.2016.2549545

Document Version
Peer reviewed version

Stable Grip Control on Soft Objects With Time Varying Stiffness

Thrishantha Nanayakkara, *Member, IEEE*, Allen Jiang, *Student Member, IEEE*, Maria D. Rocio Armas Fernandez *Student Member, IEEE,*, Hongbin Liu, *Member, IEEE*, Kaspar Althoefer, *Member, IEEE*, and Joao Bimbo *Student Member, IEEE,*

***Abstract*—Humans can hold a live animal like a hamster without overly squeezing despite the fact that its soft body undergoes impedance and size variations due to breathing and wiggling. Though the exact nature of such biological motor controllers is not known, existing literature suggests that they maintain metastable interactions with dynamic objects based on prediction rather than reaction. Most robotic gripper controllers find such tasks very challenging mainly due to hard constraints imposed on stability of closed loop control and inadequate rate of convergence of adaptive controller parameters. This paper presents experimental and numerical simulation results of a control law based on a relaxed stability criterion of reducing the probability of failure to maintain a stable grip on a soft object that undergoes temporal variations in its internal impedance. The proposed controller uses only three parameters to interpret the probability of failure estimated using a history of grip forces to adjust the grip on the dynamic object. Here we demonstrate that the proposed controller can maintain smooth and stable grip tightening and relaxing when the object undergoes random impedance variations, compared to a reactive controller that involves a similar number of controller parameters.**

I. Introduction

To date, one of the main challenges encountered in the field of robotics is to maintain the performance of controllers in an uncertain environment [1], [2], [3]. Uncertainty of the environment often causes the dynamic interactions to be metastable, wherein the states remain within a safe region most of the time, with a guarantee that there will be an instance where they depart that region given sufficient time. Grasping tasks on variable stiffness soft objects like holding a pet hamster and holding a pulsating tissue during surgery fall into this class. Control actions on such metastable grasps should be assessed based on their ability to keep the probability of failure low rather than traditional strict asymptotic stability criteria used in robust controllers.

This work was supported by the European Community's Seventh Framework Programme (FP7/2007-2013) project DARWIN (Grant No: FP7-270138) and UK Engineering and Physical Sciences Research Council grants EP/I028773/1 and EP/I028765/1.

Thrishantha Nanayakkara, Maria Fernandez, Hongbin Liu, and Kaspar Althoefer are with the Centre for Robotics Research, Department of Informatics, King's College London, Strand, London, WC2R 2LS, United Kingdom thrish.antha, allen.jiang, maria.armas_fernandez, hongbin.liu, kaspar.althoefer@kcl.ac.uk

Allen Jiang is with Auris Surgical Robotics, USA im@allenjiang.com

Joao Bimbo is with the Department of Advanced Robotics, Istituto Italiano di Tecnologia (IIT), via Morego 30, 16163 Genova, Italy joao.bimbo@iit.it

In [4], the authors have shown that the human brain learns internal models of the environment even in the presence of random disturbances. This highlights the importance of an internal mechanism to predict the consequences of the efferent motor commands even when the environment is variable. Adaptive predictive control in force field learning tasks [5] also show how the human motor system changes predictive forward models when the task dynamics change. Work done on human subjects in grasping tasks [6] show that the uncertainty of an object leads to variability even in the hand reaching trajectories. The above findings show that human motor system uses internal models of the past experiences with an object to make predictive decisions rather than being reactive in a variable environment. In robotics, such predictive methods based on the estimation of impedance parameters of the environment are proposed in disturbance observers [7] and linear estimation of environment's impedance parameters [8]. However, the performance of these methods depends on the adequacy of the speed of convergence of model parameters relative to the rate of change of object's impedance parameters [9].

Solutions to manipulation in uncertain tasks such as non-linear model tracking for flexible arms with parametric uncertainty [10] [11], sliding mode control of robotic arms in uncertain environments [12], and time varying impedance center to adaptively change the desired impedance [13] impose a demanding computational burden on the real-time controller. Hybrid position/force control has been established by groups such as the NASA Jet Propulsion Laboratory (JPL), where in [9], a set of stability criteria were made for a known manipulator on a variable environment. However, the authors agree that a trade-off between stability and accuracy of control exists.

2D and 3D imaging has been used to determine optimal grasping locations on a target object of uncertain shape [14] and [15] uses vision when the object is deformable. However, vision cannot provide a solution to objects that undergo internal impedance variations. Other groups use active sensing, with [16], [17], [18] employing tactile sensors on the fingers and [19] examining joint torques to develop a model of the uncertain object. The third approach is to use historical data or learning to develop better grasps. This approach ranges from object templates with pre-calculated optimal grasps [20] to primitives and reinforcement learning [21]. A method to control the grasp force on a rigid object based on past knowledge of stick-slip distributions has been proposed in

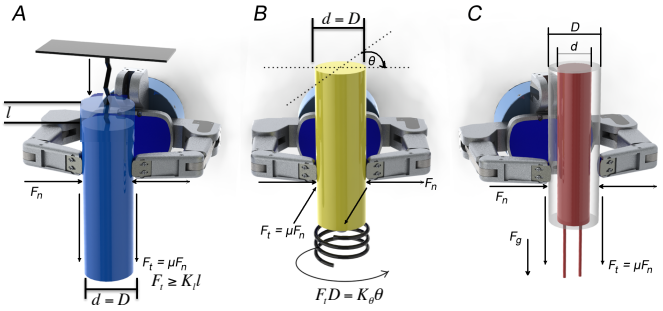

Fig. 1. The Barrett hand gripping a variable object in three different scenarios. A) The variable impedance object is pulled against a counter force (e.g. a pulsating artery is pulled by a robotic gripper in a minimally invasive surgery). B) The object is rotated against counter torque (e.g. a lung tissue is twisted by a robotic gripper to open a site covered by it in a minimally invasive surgery, twisting a doorknob, wringing a wet towel, or turning a key, where the stiffness is not uniform over the twisted angle). C) The object changes diameter by inflation.

[22]. Including our recent work [23], methods to identify parameters of friction models by interacting with rigid objects have been studied elsewhere [24]. However, to the best of our knowledge, this is the first time a mathematical model is proposed to control the grip forces on a variable impedance object by estimating the probability of failure. We presented the preliminary work in [25]. In this paper, we provide new derivations to establish a criterion to reduce the probability of failure, and provide extensive analytical results.

In this paper, we propose a novel controller that uses a realtime estimate of the standard deviation of a pinch grip force on a variable stiffness soft object to compute a biased probability of failure in order to adjust the level of grip. The proposed controller uses only three design variables - 1) a bias parameter that determines the relative gradient of grip tightening vs relaxing when the probability of failure increases vs decreases, 2) a safety threshold parameter that determines the buffer added on top of a critical grip force to maintain safe grip forces when the object goes through stiffness variations, 3) a sensitivity parameter that determines the rate of grip update when the probability of failure varies. Therefore, this proposed controller is simple enough to be compared with a PID controller of three parameters except that the proposed controller allows a designer to 1) bias the sensitivity to increases and decreases of the probability of failure, 2) take the historical behavior of the object into account to update the computation of the probability of failure, whereas in a PID controller there is no bias for positive or negative errors nor any regard for the historical behavior of the object to interpret grip force errors.

The rest of the paper is organized as follows. Section II defines the problem and provides analytical insights into the derivation of the grip controller on a variable impedance object. We show numerical simulation and experimental results with comparisons to confirm the effectiveness of the proposed method in section III. Finally, section IV provides concluding remarks.

II. Probabilistic Expectation of Failure as a Feedback Signal to Control Grip Force

The problem addressed in this paper is to maintain a pinch grip without any resort to use form closure on a soft cylinder with stiffness and damping parameters undergoing random variations. Real-life applications can range from holding a pulsating artery during minimally invasive surgery, holding live animals like hamsters, to industrial maintenance of liquid transporting tubes. In our numerical simulations we limit the impedance parameter variation to a Gaussian distribution. However, we show that the controller performs well even in a non-Gaussian scenario.

Figure 1 shows three scenarios of manipulating a variable cylinder. In the case of pulling a cylinder against a linear spring of stiffness K_l by a length l in Figure 1 (A), the tangential friction force F_t should meet the condition given by

$$\begin{aligned} F_t &\geq K_l l \\ F_n &\geq \frac{K_l l}{\mu} \end{aligned} \tag{1}$$

where, μ is the coefficient of static friction.

In the case of rotation of a cylinder of nominal diameter D against a spring of stiffness K_θ in Figure 1 (B), the tangential friction force F_t at a gripper finger gap d ($d \leq D$) and rotation θ, should meet the condition given by

$$\begin{aligned} F_t(D-d) &\geq K_\theta \theta \\ F_n &\geq \frac{K_\theta \theta}{\mu(D-d)} \end{aligned} \tag{2}$$

In the variable radius case in Figure 1 (C), gravity F_g pulls the cylinder. Thus, the condition is given by

$$\begin{aligned} F_t &= F_g/2 \\ F_n &\geq \frac{F_g}{2\mu} \end{aligned} \tag{3}$$

Therefore, the common criterion to maintain grip is given by

$$F_n \geq F_n^* \tag{4}$$

where, F_n^* is a critical normal force that should be determined apriori. Any controller using a reference point, such as PID, requires us to know this critical force F_n^* that can be easily determined using few apriori experimental trials and updated every time a grip failure occurs. In the experiments, we first obtain an initial estimate by gripping the object with finger aperture set at the nominal diameter of the object. The robot holds the object that undergoes random inflation/deflation without any grip control till a failure occurs. We take the force at grip failure to be the initial estimate of F_n^*.

A. Computing a probability of failure for a pinch gripper

The gripping of a variable impedance object is a metastable task, wherein the system is not always truly stable due to the random variations within it. Thus, the Lyapunov type stability does not strictly apply to this class of systems, making a formal proof for stability difficult to address.

Let $V(k) = P(k)^2$ be a candidate positive definite Lyapunov function, where $P(k)$ is the probability of failure at sample step k. Then for stability, $V(k) - V(k-1) < 0$ for all k. This leads to the condition:

$$\begin{aligned} P(k)^2 - P(k-1)^2 &< 0 \\ P(k) &< P(k-1) \end{aligned} \tag{5}$$

This Lyapunov requirement for a monotonic reduction of the probability of failure can never be guaranteed in a metastable system, and is in fact not needed. Instead, we use a relaxed condition like keeping the probability of failure below a given threshold.

Let us assume that normal force F_n exhibits a Gaussian variation given by

$$g(F_n) = \frac{1}{\sqrt{2\pi}\sigma_{F_n}} \exp\left(-\frac{(F_n - \bar{F}_n)^2}{2\sigma_{F_n}^2}\right) \tag{6}$$

where $\bar{F}_n$ is the expected value of F_n and $\sigma_{F_n}^2$ is the variance of F_n in a general case where the nominal diameter of the tube D, and the distance between the fingers of the gripper d undergoes variations such that $d \leq D$.

Then, the probability of the normal force F_n falling below a β distance from the critical force F_n^*, is given by

$$P(F_n < F_n^* + \beta) = \int_0^{F_n^*+\beta} g(F_n) dF_n \tag{7}$$

The limits of equation (7) can be re-written as given by

$$P(F_n < F_n^* + \beta) = \int_{(\frac{F_n^*+\beta}{2})-(\frac{F_n^*+\beta}{2})}^{(\frac{F_n^*+\beta}{2})+(\frac{F_n^*+\beta}{2})} g(F_n) dF_n \tag{8}$$

Following the mean value theorem of definite integrals of Gaussian density functions [30], there is an ε $(0 < \varepsilon < \beta)$, so that the above integral in equation (8) can be simplified to the difference between the limits of the integral $\left[\left((\frac{F_n^*+\beta}{2}) - (\frac{F_n^*+\beta}{2})\right) - \left((\frac{F_n^*+\beta}{2}) + (\frac{F_n^*+\beta}{2})\right) = F_n^* + \beta\right]$ multiplied by $g(\varepsilon)$ as given in

$$P(F_n < F_n^* + \beta) = \frac{F_n^* + \beta}{\sqrt{2\pi}\sigma_{F_n}} g(\varepsilon) \tag{9}$$

It should be noted in equation (7) that β can inflate the probability of "failure" by providing a conservative margin on top of the true failure point when F_n falls below the critical force F_n^*. Moreover, β serves as a correction for the uncertainty of experimental estimation of F_n^*. In the experiments, we estimated the critical force F_n^* by gradually relaxing the grip on the variable impedance object till the object was dropped. We took the average of the grip force just before the failure as an initial estimate of the critical force. Findings on how humans manage grip forces during in-hand manipulation of objects indicate that the brain uses internal models of the object dynamics to estimate safety margins for grip forces that are updated during manipulation [29]. Here, in this case, our initial guess of F_n^* somewhat similar to that process. However, a machine learning approach based on a Bayesian model to update F_n^* will be the focus on future research.

Now let us consider an arbitrary feedback controller in the form given by

$$d(k+1) = d(k) + \eta z \tag{10}$$

where d is the distance (aperture) between the two fingers, η is the grip adaptation rate, and z is an arbitrary feedback variable related to the probability of failure.

Then, this control law will lead to a stable grip if the expected value of grip force over a finite horizon increases when the probability of failure increases and vice versa.

Let us apply the control law on an object with a variable internal stiffness K.

The grip force at time k and $k+1$ are given by

$$F_n(k) = K(k)(D - d(k)) \tag{11}$$

$$F_n(k+1) = K(k+1)(D - d(k+1)) \tag{12}$$

Substituting $d(k+1)$ from equation (10) in (12),

$$\begin{aligned} F_n(k+1) &= K(k+1)(D - (d(k) + \eta z)) \\ &= K(k+1)((D - d(k)) - \eta z) \end{aligned} \tag{13}$$

By subtracting equation (13) from (11), we obtain the incremental force given by

$$\Delta F = (\Delta K)(D - d(k)) - K(k+1)\eta z \tag{14}$$

Taking the expected value of both sides of equation (14),

$$E[\Delta F] = E[(\Delta K)(D - d(k))] - E[K(k+1)\eta z] \tag{15}$$

Since stiffness variation is independent from grip aperture, we can write equation (15) as given by

$$E[\Delta F] = E[\Delta K] E[(D - d(k))] - \eta E[K(k+1)z] \tag{16}$$

Assuming the stiffness variation of the object follows a Gaussian distribution, $E[(K(k+1) - K(k))] \approx 0$ for a finite horizon.

Then equation (16) can be re-written as

$$\begin{aligned} E[\Delta F] &= -\eta E[K(k+1)z] \\ &= -\eta E[K(k+1)] E[z] \\ &= -\eta \overline{K} E[z] \end{aligned} \tag{17}$$

where $\overline{K}$ is the expected value of tube stiffness, which is a positive value.

Therefore, in order to obtain a positive expected value for the incremental force when the probability of failure increases, and vice versa, we can write z as given by

$$z = -(P(F_n < F_n^* + \beta) - \delta) \tag{18}$$

where $0 < \delta < 1$ is a controller design parameter to choose how conservative the control effort should be. For instance, if δ is chosen to be small, then the controller is "stricter", requiring a very low probability of failure to relax the grip. In other words, δ biases the controller to interpret the probability of failure to take a decision to increase or decrease the grip.

Hence by substituting z from equation (18) in equation (10), the final stable controller is given by

$$d(k+1) = d(k) - \eta(P(F_n < F_n^* + \beta) - \delta) \tag{19}$$

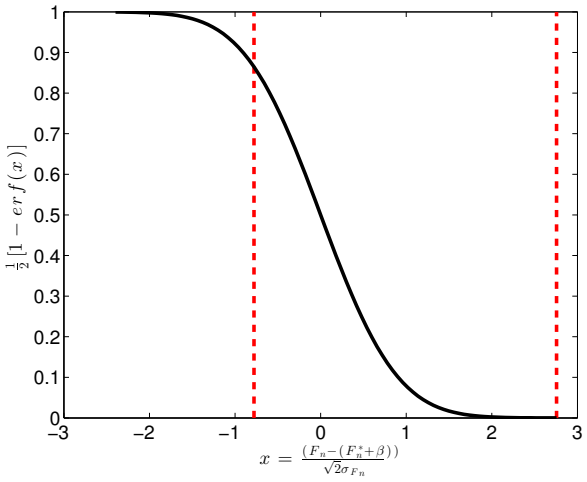

Fig. 2. Plot of the probability computation in equation (20) based on the σ_{F_n} found in the experimental results. The dashed vertical lines demarcate the range of the input $\frac{(F_n-(F_n^*+\beta))}{\sqrt{2}\sigma_{F_n}}$ in the experiment.

We used the standard error function for real-time computation of the probability of failure [31] given by

$$P(F_n < F_n^* + \beta) = \frac{1}{2}\left[1 - erf\left(\frac{(F_n - (F_n^* + \beta))}{\sqrt{2}\sigma_{F_n}}\right)\right] \quad (20)$$

where erf stands for the error function, which is related to the cumulative distribution or the integral of the standard normal distribution. Figure 2 shows the shape of $\frac{1}{2}\left[1 - erf\left(\frac{(F_n-(F_n^*+\beta))}{\sqrt{2}\sigma_{F_n}}\right)\right]$ in equation (20) for the σ_{F_n} found in the experimental data for the grip force F_n. Since $\beta > 0$ inflates the probability of failure, $P(F_n < F_n^* + \beta)$ serves as a likelihood of failure. It becomes an instantaneous probability of failure when $\beta = 0$. The major advantage of this controller is that it does not require to know the impedance parameters of the object. Rather, a memory of past normal forces is enough to compute the variance of interaction forces. In this case, we took the whole history of forces up to any given time to compute σ_{F_n} since it accounts for the total range of interactions experienced by the gripper. We set the grip adaptation rate to be $\eta = 0.0001$ in this case.

Now, let us investigate the relationship between the upper bound of the safety margin β and the standard deviation of the variability of the experienced normal force σ_{F_n}.

We take the derivative of the probability given in equation (9), given by

$$\begin{aligned} &\frac{\partial P(F_n < F_n^* + \beta)}{\partial \sigma_{F_n}} \\ &= \frac{\partial}{\partial \sigma_{F_n}}\left[\frac{F_n^* + \beta}{\sqrt{2\pi}\sigma_{F_n}} \exp\left(-\frac{\varepsilon^2}{2\sigma_{F_n}^2}\right) + \overline{F_n}\right] \\ &= \frac{F_n^* + \beta}{\sqrt{2\pi}\sigma_{F_n}^2} \exp\left(-\frac{\varepsilon^2}{2\sigma_{F_n}^2}\right)\gamma \end{aligned} \quad (21)$$

where $\gamma = \left(\frac{\varepsilon^2 - \sigma_{F_n}^2}{\sigma_{F_n}^2}\right)$ and $\overline{F_n}$ is the expected value of the grip forces so that $\frac{\partial \overline{F_n}}{\partial \partial \sigma_{F_n}} = 0$.

Equation (21) shows that the probability of failure for a given safety margin β decreases when σ_{F_n} increases, only if $\frac{\partial P(F_n < F_n^* + \beta)}{\partial \sigma_{F_n}} < 0$. Since $\frac{F_n^* + \beta}{\sqrt{2\pi}\sigma_{F_n}^2} \exp\left(-\frac{F_n^2}{2\sigma_{F_n}^2}\right) > 0$, $\forall \beta > 0$, $\forall \varepsilon$ in equation (21), this condition can be satisfied if $\gamma < 0$.

This leads to the condition $\varepsilon \leq \sigma_{F_n}$. Since $0 < \varepsilon < \beta$, this condition for a stable grip can be guaranteed by $\beta \leq \sigma_{F_n}$.

Based on the above insights, we propose that an estimate of the probability of failure in equation (9) for $\beta > 0$, can be used as a feedback signal to control the grip on the variable impedance object. Moreover, we set $\delta = 0.3$ in the following numerical simulations and experiments.

The proposed controller was compared with a PID control law given in equation (22) (for simulations) for different settings of parameters.

$$d(k+1) = d(k) + \left[P_{sim}F_e + D_{sim}\dot{F}_e + I_{sim}\sum_{i=0}^{i=k} F_e\right] \quad (22)$$

where, $F_e = (F_n - (F_n^* + \beta))$, P_{sim}, D_{sim}, and I_{sim} are P-gain, D-gain, and I-gain used in the simulations, i is the sampling step count, and k is the present sampling step.

We used the same PID control law in the experiments. For clarity, we use different notations for PID parameters as shown in equation (23).

$$d(k+1) = d(k) + \left[P_{exp}F_e + D_{exp}\dot{F}_e + I_{exp}\sum_{i=0}^{k} F_e\right] \quad (23)$$

where, P_{exp}, I_{exp} and D_{exp} gains were experimentally set to 0.35, 0.02 and 0.02 respectively, for best performance.

III. Results

Before proceeding to results, let us discuss the essential difference between the proposed controller given in equation (19) and the PID controller given in equations (22) for simulation and (23) for experiments. In the proposed controller, the error of a given grip force F_n compared to a reference $F_n^* + \beta$ is given a context dependent interpretation using the probability of failure that changes depending on the shape of the Gaussian distribution of F_n itself. However, in PID control, the grip force error is given a uniform meaning across different contexts of the object. Moreover, the parameter δ in the proposed controller allows a designer to change the bias of the controller to grip or relax with the changes of failure probability reduces. For instance, lower values of δ will make the controller grip more when the failure probability increases, but relax less when failure probability reduces by the same amount. PID controller does not allow us to design such a bias.

A. Simulation results

Algorithm 1 shows the procedure taken to simulate the proposed controller and the PID controller under different conditions. The actual servo control details of the Barrett hand were not available. Therefore, lines 19 and 20 of algorithm 1 model the internal servo controller of the motors used to control the robotic gripper.

Algorithm 1 Algorithm for pinch grip control on a soft object with variable impedance and nominal diameter

<Initialize parameters>
Set parameters in the first column of table I
<Initialize variables>
$x \leftarrow (D-a)$ ▷ Desired compression of the soft object. Set initial $a = 20$ mm.
$\hat{x} \leftarrow x$ ▷ Set current compression realized by the robot $\hat{x}$ to be x.
$F_n \leftarrow Kx + C\dot{x}$ ▷ Compute grip force
for <Set length of time> **do**
  if time = n/f **then** ▷ Frequency f as in table I, $n = 1,2,3,\cdots$.
    $K \leftarrow N(\bar{K}, \sigma_K^2)$ ▷ $N()$ is the normal random number generator.
    $C \leftarrow N(\bar{C}, \sigma_C^2)$
    $D \leftarrow D_o + \zeta(K - \bar{K})$ ▷ $\zeta = 0$ if D is uniform. $\zeta = 10^{-5}$ for moderate variability in D. $\zeta = 5 \times 10^{-5}$ for high variability in D.
  end if
  Compute σ_{F_n} from the history of F_n.
  Compute $P(F_n < F_n^* + \beta)$ in eq. 19 using the error function.
  Update a from eq. 19 if proposed controller is simulated
  Update a from eq. 22 if PID controller is simulated
  $x \leftarrow (D-a)$ ▷ Desired compression
  $e = \hat{x} - x$ ▷ Compute the grip error
  Simulate the robot's grasp controller using the state equation $\dot{e} = Ae + Bu$, where $A = -K/C$, $B = 1/C$, and u is the control command.
  Compute $u = -Ge$ ▷ G is the optimal gain obtained from the linear quadratic regulator function in Matlab
  $\hat{x} \leftarrow x + e$ ▷ Obtain e by integrating $\dot{e}$
  if Time = 10 sec **then**
    Change $\bar{K}$, σ_K^2, $\bar{C}$, σ_C^2, and f to the second column of table I
  end if
  if $F_n < F_n^*$ **then**
    Terminate ▷ Grip force is not enough
  end if
end for

1) Statistical summary of the behavior of the proposed controller and the PD controller for a variable impedance cylinder with variable nominal diameter: The following table I shows all the relevant parameters found from the experimental results.

TABLE I
SIMULATION CONDITIONS.

Tube variables	First 10 sec	Second 10 sec
Impedance variation frequency (f)	0.5 Hz	1 Hz
Average stiffness ($\bar{K}$)	263.3 N/m	259.3 N/m
Standard deviation of K (σ_K)	19.3 N/m	30.8 N/m
Average damping $\bar{C}$	1571.9 Nsec/m	1535.6 Nsec/m
Standard deviation of C (σ_C)	218.62 Nsec/m	344.56 Nsec/m
Initial diameter of the tube D_o	24.63 mm	24.63 mm
F_n^*	1 N	1 N
η	1×10^{-4}	1×10^{-4}

We conducted simulations for a range of possible levels of variability of D for the conditions shown in table I to quantify the average time taken to failure and its variability. In this study, we conducted 100 trials for a given level of variability of D. This was repeated for 20 levels of variability in D. Simulation time was limited to 20 seconds to highlight the behavior around the 10 second mark where the tube stiffness variation frequency changes from 0.5Hz to 1Hz. Therefore flat failure time at 20 seconds in some plots correspond to "infinite" failure time for practical purposes. The integral gain I_{sim} was set to zero in all simulations because there is little interest in the steady state accuracy in this application where the tube frequently undergoes stiffness variations. From figure 3, we can notice that the time to failure reduces with increasing standard deviation of variations in D. It should be noted that the performance significantly improves with a reduction of δ from 0.3 to 0.2 for $\beta = 1$ ($p < 0.006$, multivariate ANOVA test). If we consider 10 sec as a reference point of failure, where the frequency of impedance variation transits from a low 0.5 Hz to a high rate 1 Hz, we notice that the case of $\delta = 0.2$ can afford to have a standard deviation of D at 2.3 mm in contrast to 1.4 mm in the case of $\delta = 0.3$. We also note that the improvement is not linear. When the variability of D increases, the improvement due to a reduction of δ makes relatively higher improvements at larger variability of D.

Obviously, the effect of β on the performance is very significant ($p < 0.001$, multivariate ANOVA test). An increase of β from 1 to 2 manages to keep the time to failure above 10 sec for both cases of δ. The multivariate ANOVA test showed that there is no statistically significant influence from the interaction effect between δ and β on the failure time ($p > 0.1$, multivariate ANOVA test). This finding also highlights that β and δ can be treated as two independent parameters in the controller. In general, these observations further confirm the effectiveness and flexibility of the proposed controller that allows to give a relative interpretation to the probability of failure by choosing appropriate levels of δ and β.

Figure 4 shows how the time to failure behaved for different values of the grip adaptation rate η. We notice that when it reduced from $\eta = 0.0005$ to 0.0001, the curve shifted up

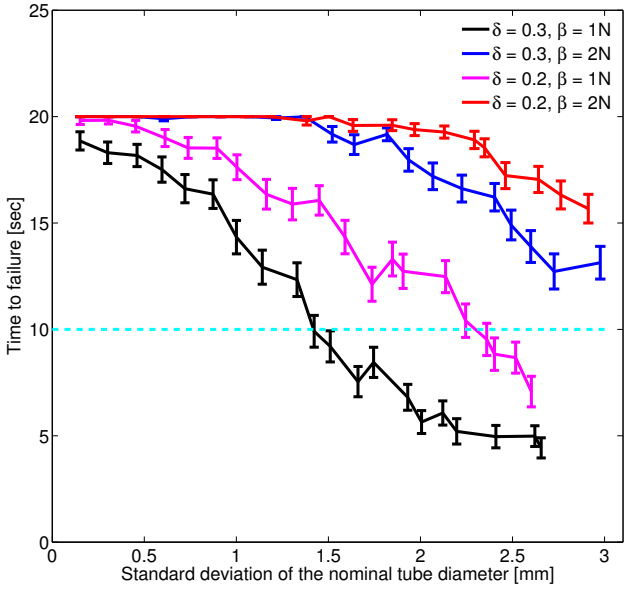

Fig. 3. Behavior of time to failure for the proposed controller on a soft tube that undergoes temporal impedance variation with different levels of variability in D. Each error bar corresponds to 100 trials. For each pair of δ and β, batches of 100 trials were repeated for 20 levels of variability in D for $F_n^* = 3$N. The cyan horizontal dashed line shows the time at which the frequency of impedance variation changed from 0.5 Hz to 1 Hz.

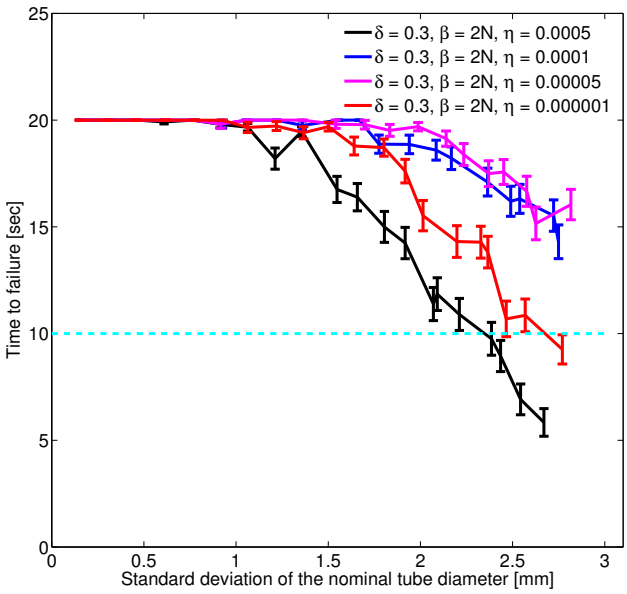

Fig. 4. Behavior of time to failure for the proposed controller for different values of η for $\delta = 0.3$ and $\beta = 2$ N. All other conditions were identical to those in figure 3.

significantly ($p < 0.00001$, Mann-Whitney U-test for non-Gaussian distributions). However, when it further reduced to 0.00005, the curve did not show a statistically significant upward shift ($p > 0.5$), though there is a slight visual effect of shifting upwards. When it reduced to 0.000001, the curve started to shift downwards. These observations suggest that the grip adaptation rate η does have a significant effect on the failure rate when it is at a high range $\eta > 0.0001$, and the sensitivity drops in a large range of small values $0.000001 < \eta < 0.0001$. However, this range also depends on the randomly varying object itself. Therefore, our recommendation is to tune this design variable starting from a small value.

In figure 5 we notice that the stability of the PID controller reduces at high variability in the nominal tube diameter on top of the variation in impedance parameters. The stability improves for low P_{sim} and D_{sim} parameters, though it settles down at a maximum level of stability. Multivariate ANOVA test showed that the P_{gain} does not have a statistically significant impact on the time to failure ($p > 0.3$), while the D_{gain} does ($p < 0.008$).

Comparing the "infinite" time to failure regions (the flat region of certain curves) we notice that the best case in figure 4 for the proposed controller extends to 1.7 standard deviation of D whereas that in figure 5 for the PID controller is 1. This shows superior stability of the proposed controller.

B. Experimental results

Figure 6 shows the experimental setup where the variable stiffness tube was gripped by a ROS-operated Barrett hand with two ATI Nano17 F/T sensors attached to the fingers. Two variable stiffness tubes were tested, with different stiffness properties. In all experiments, the controllers were run at 100Hz. The custom fingertips have been developed in [26]. The finger consists of a 6-axis force/torque sensor (ATI Nano17, resolution = 0.003 N, sampling rate = 100 Hz) and a hemispherical fingertip. The fingertip was made of the rigid ABS (Acrylonitrile butadiene styrene) plastic material and has a diameter of 18 mm. A contact sensing algorithm to allow the fingers to accurately estimate the instantaneous friction force and the normal force was developed in [26]. The estimation errors of normal force and friction force were less than 0.04N for the rigid finger. It has also been shown in [27], the contact sensing algorithm can also be extended to fingertip covered with soft layers, allowing the proposed controller work for compliant fingertips as well.

We show experimental results of two rubber tubes that were randomly inflated and deflated, changing its internal impedances, using an air compressor and an SMC ITV0030-3BS-Q pressure regulator. The internal pressure varied between 0 kPa and 217 kPa (gauge pressure), changing its diameter and stiffness according to random inputs that followed a Gaussian distribution.

Since the standard deviation of the variation of diameter of both tubes were found to be in the range $0.7 - 1.2$, we conducted experiments with $\delta = 0.3$ and $F^* + \beta = 2$N was chosen after several experiments.

The distance between the contacts was obtained from the forward kinematics of the Barrett Hand together with the contact sensing method described in [28].

In order to evaluate the performance of the proposed controller, a comparison was made to a tuned PID controller. The main reason as to why we use a PID controller to

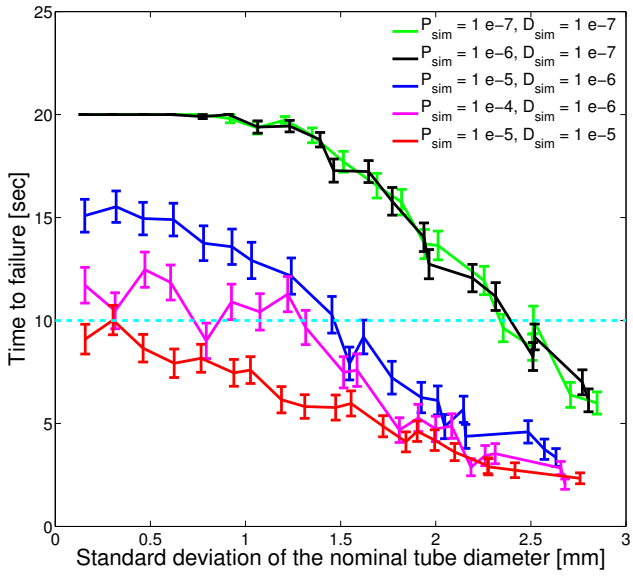

Fig. 5. Behavior of different PID grip force controllers for various levels of variability in the nominal tube diameter in addition to Gaussian variation in impedance parameters. For simplicity, I_{sim} was set to zero. Each error bar corresponds to 100 trials. For each pair of δ and β, batches of 100 trials were repeated for 20 levels of variability in D. The cyan horizontal dashed line shows time at which the frequency of impedance variation changed from 0.5 Hz to 1 Hz. The exponent $1e-N$ denotes 1×10^{-N}

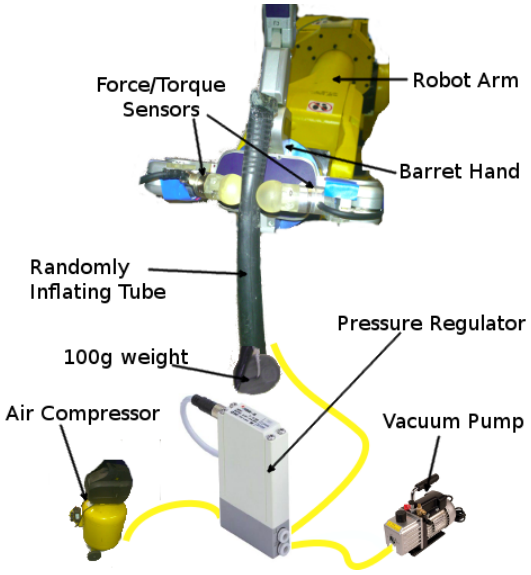

Fig. 6. Experimental Setup Diagram

compare results is that it has a comparable number of parameters, whereas many other more complicated controllers like adaptive-predictive controllers use larger number of parameters that have to be manually tuned or adapted real-time. Moreover, the order selection (the number of historical samples of the state to be used to make a prediction) of those controllers require a lot of effort. Therefore, by using a PID controller which too requires tuning of parameters, we can compare the performance of the proposed controller given

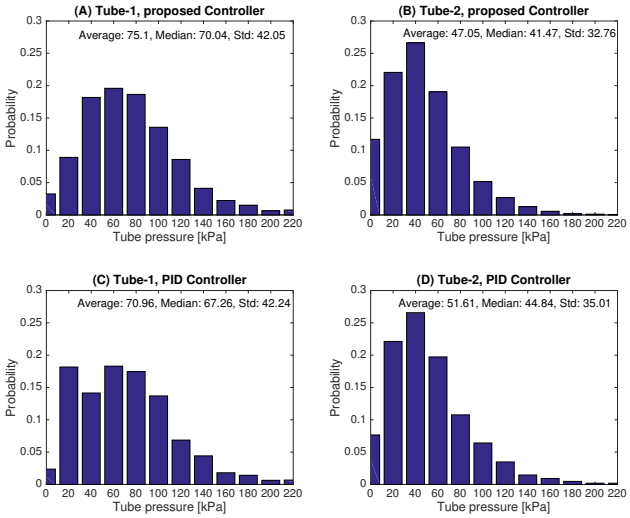

Fig. 7. Overall distribution of pressure variation in each tube under the proposed and PID controllers.

comparable user-friendliness.

The input for both controllers was the normal force, obtained through an intrinsic tactile sensing scheme [28]. The command on the robot fingers was a velocity command, which is converted to a motor torque by the Barrett Hand's internal micro-controller.

The proposed controller was tested in 66 trials for tube-1 and 38 trials for tube-2, and the PID controller was tested in 9 trials for the tube-1 and 12 trials for tube-2. In each trial, the frequency of variation of internal pressure of the tube was increased in steps and then decreased in the same steps to test the performance of the grip controllers under different statistical conditions. However, there was no statistically significant difference in the overall variability of pressure (figure 7, $p > 0.5$, Mann-Whitney U test) between the two controllers for each tube.

The standard deviations of the nominal tube diameters corresponding to the pressure distributions in figure 7 were 3.23, 2.71, 2.19, and 2.27, for the tube-1 under proposed controller, tube-1 under PID control, tube-2 under the proposed controller, and for the tube-2 under PID control. Therefore, the experimental conditions fall within the upper range of variability in nominal tube diameter considered in the simulations (figures 3, 4, and 5).

Figure 8 shows the experimental results for the proposed controller in a representative trial. The proposed controller did not fail in all 66 trials on the tube-1. Subplot (A) shows how the frequency of tube pressure was changed from $2 \rightarrow 4 \rightarrow 8 \rightarrow 4 \rightarrow 2$ Hz. The corresponding pressure profiles are shown in subplot (C) that varies with a mean 75.1kPa and a standard deviation of 42.05. Subplot (B) shows the estimated probability of grip failure. It should be noted that the probability of failure in this case is an inflated estimate of the true probability of failure due to the use of β in the calculation. Therefore, a failure probability of 1 does not mean a certain failure. This is also evident in the fact that all grip

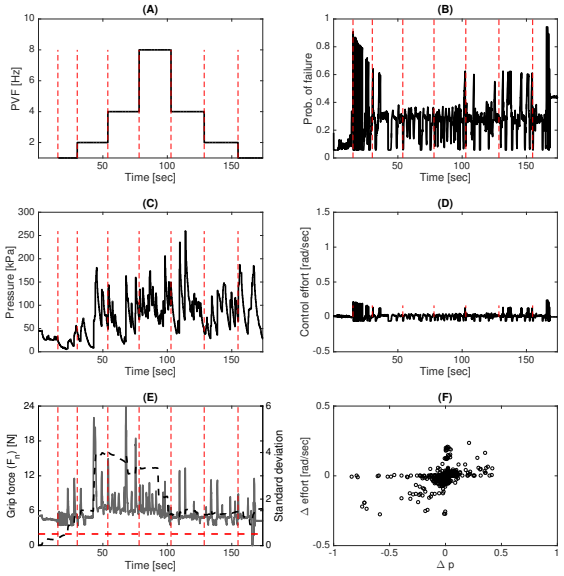

Fig. 8. A representative trial for the tube-1 under the proposed controller. The red dashed vertical lines mark where the changes in the frequency of tube pressure variations occur. In subplot (E) the left and right y-axes correspond to the grip force and its standard deviation respectively. The red dashed horizontal line shows the critical force. The black dashed line shows the variation of the standard deviation of the grip force.

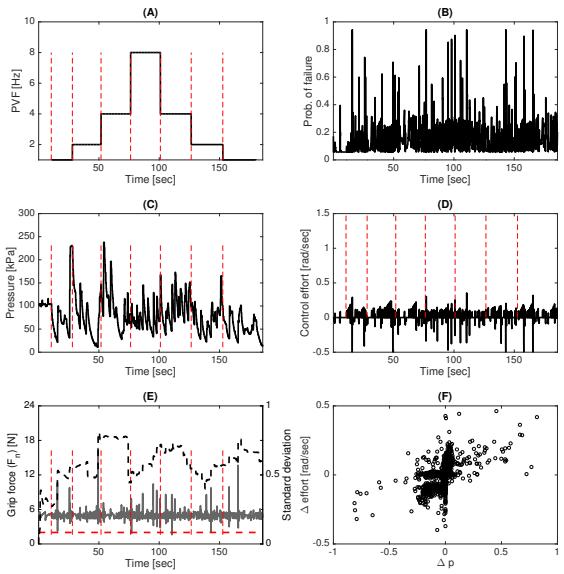

Fig. 9. A representative trial for tube-1 under the PID controller. The red dashed vertical lines mark where the changes in the frequency of tube pressure variations occur.

forces in subplot (E) are well above the threshold even where the failure probability is high. The variation of σ_{F_n} shown in subplot (E) was computed using a moving window of 500 samples. From figure 8 (E) we can see that sudden large peaks of grip force increases σ_{F_n} that leads to higher sensitivity of failure probability estimates (see equation (20) and figure 2)

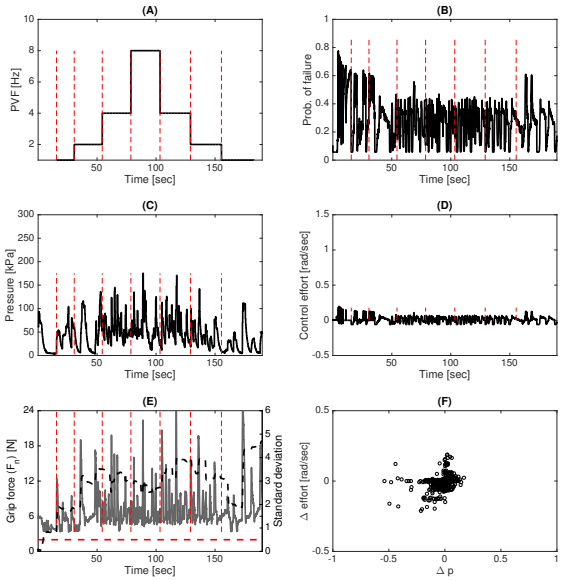

Fig. 10. A representative trial for tube-2 under the proposed controller. The red dashed vertical lines mark where the changes in the frequency of tube pressure variations occur.

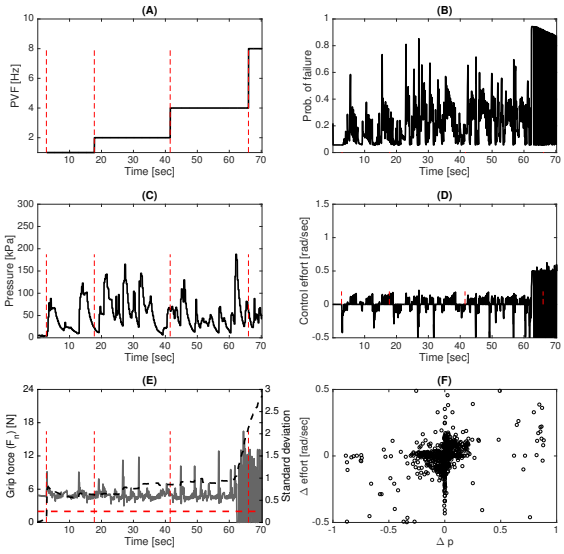

Fig. 11. A representative trial for tube-2 under the PID controller. The red dashed vertical lines mark where the changes in the frequency of tube pressure variations occur.

to the drops in grip force. This leads to several subsequent peaks in grip forces between due to the elevated sensitivity of the grip controller given in equation (19). Subplot (D) shows the control effort (speed command) which represents the power consumed to control the grip. Subplot (F) shows how the changes of this control effort are related to the changes of probability of failure. We notice that drops of failure probability and corresponding drops of effort are larger

than their increases.

Figure 9 shows the experimental results for the tuned PID controller in a representative successful trial. In addition to larger probabilities of failure in subplot (B) compared to that of figure 8, we can also notice in subplot (F) that the change of control effort in response to the change of failure probability is noisier under the proposed controller. The PID controller has no mechanism to make use of the variation of σ_{F_n} (dashed line in figure 9(E)) due to its pure reactive nature. Due to this, subplot (B) shows higher probability of failure compared to the corresponding plot in figure 9.

Figure 10 shows representative experimental results for the proposed controller on tube-2. The proposed controller did not fail. However, the corresponding results for PID controller shows that it failed at 8Hz in this particular trial at about 70 seconds (figure 11).

The proposed controller failed 0% in tube-1, 9% in tube-2, and the PID controller failed 0% in tube-1 and 17% in tube-2.

Figure 12 summarizes the response patterns of the two controllers on the two tubes across all trials. The proposed controller was tested for $\delta = 0.2, 0.3$ and 0.4 to show the effect of this design parameter that biases the controller in the range of failure probabilities. We can notice that the average probability of failure for the proposed controller is smaller for both types of tubes ($0.28, 0.42, 0.48$ for tube-1 and $0.29, 0.43, 0.49$ for tube-2 for the three values of δ, compared to 0.53 and 0.54 in the PID controller). When δ approaches 0.5, the proposed controller approaches the unbiased behavior of the PID controller with an accompanying increase in the probability of failure. This behavior can also be seen in figure 13 where we show the change of control effort against the change of probability of failure. The average control effort is the same for both controllers. However, its variability is larger for PID compared to the proposed controller (PID having a standard deviation of 0.07 [rad/sec] and 0.08 [rad/sec] for tube-1 and 2 while that for the proposed controller is $0.03, 0.05, 0.06$ [rad/sec] for tube-1 and $0.04, 0.05, 0.06$ [rad/sec] for tube-2 for the three values of δ). Moreover, the incremental relationships in figure 13 show that the proposed controller has more tendency to reduce probability of failure and accompanying reduction of control effort at low values of δ compared to the symmetric behavior of the PID controller. The average grip force for the proposed controller is slightly higher for both tubes (6.02N and 6.67N for tube-1 and 2 for $\delta = 0.2$ compared to 4.71N and 4.48N for the PID controller). However, we notice that the grip forces in the proposed controller approach the PID range when δ is increased beyond 0.3. When δ was increased from 0.2 to 0.3, the average diameter of tube-1 increased from 15.61mm to 18.61mm indicating that the increase of δ amounts to a relaxation of the controller. This was also true for tube-2. The summary of all key values are given in table II.

It should be noted in figure 13 that the proposed controller has a less noisy response to changes in failure probability compared to the PID controller, which is also evident by the lower variance of control effort in figure 12. This comes from

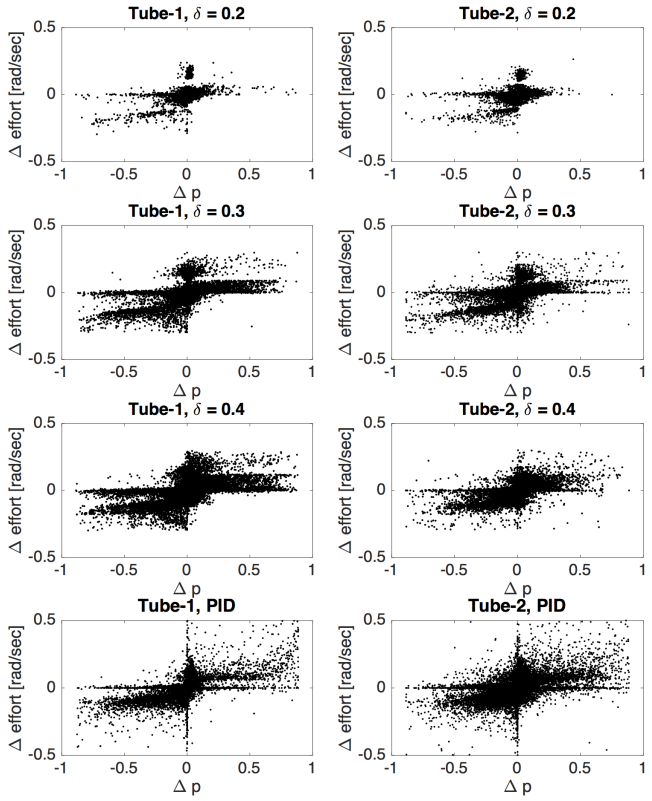

Fig. 13. Change of control effort in response to change of failure probability in the proposed controller and that in response to change of grip force error in the PID controller for both tubes.

the parameter δ that biases the proposed controller to tighten the grip when the probability of failure increases but does not relax by the same amount for the same drop in probability of failure. This ability to control the bias gives an added advantage to the proposed controller with just two parameters to be tuned - β and δ.

IV. Conclusion

Despite many advancements in robust control algorithms, industries still prefer to use conventional PID controllers for robotic grippers mainly due to their simplicity and fewer number of parameters to be tuned. This study was focused on testing an alternative approach that uses a comparable number of parameters that build in an ability to interpret the grip force errors relative to its context by using an estimate of the probability of failure given a grip force. We showed here that the proposed controller performs better than tuned PID controllers for a number of configurations of the parameters. In particular, the proposed controller had a higher time to failure when the nominal diameter of the tube was variable on top of the variability of the internal impedance parameters. This superior performance comes from the fact that the probability of failure computation of the proposed controller uses a Gaussian map from the force error to the probability, whereas a PID controller uses the error as it is, causing it to be reactive when the object undergoes random temporal variations in internal impedance and nominal tube

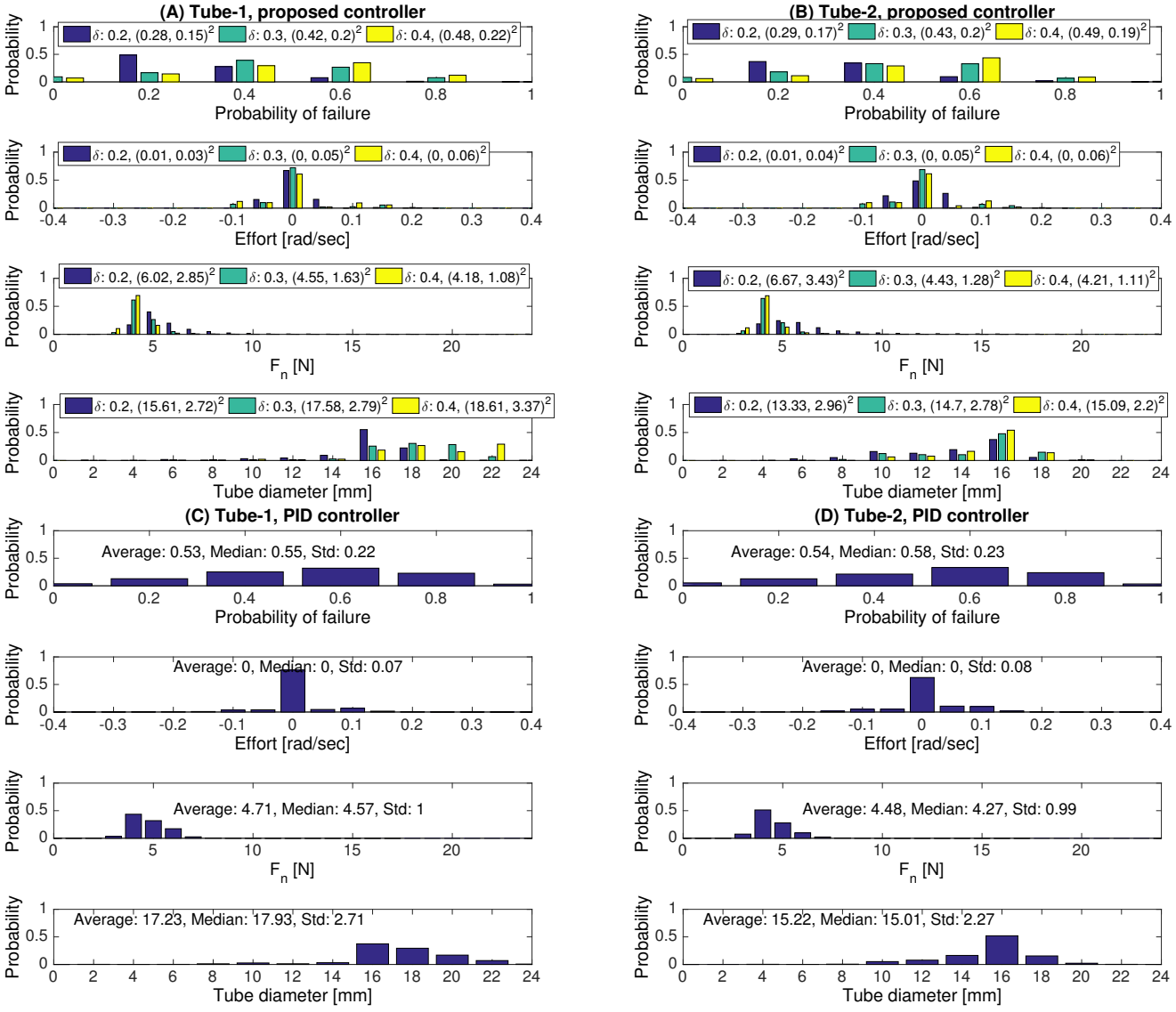

Fig. 12. Summary of 125 trials in total. Tube-1: 9 trials with PID and 66 trials with the proposed controller. Tube-2: 12 trials with PID controller and 38 trials with the proposed controller.

diameter. Moreover, the PID controller views the desired safe threshold force as a reference to be maintained whereas the proposed controller views it as a lower bound to be maintained. This leads to the PID controller to demonstrate more symmetry of grip forces around the average force than the proposed controller. This poses higher risks to the PID controller when the uncertainty of the object increases. This phenomenon is also seen in the probability distributions of the experimental grip forces experienced by the two controllers in figure 12.

This study was limited to a pinch grip typically used in many industrial applications. This is the most difficult grasping mode for a dynamic object because it does not offer the advantage of form closure in a multi-fingered grasp. However, this controller can be extended to a multi-fingered grasp by treating each finger in contact with the object to form a pair with the thumb to perform pinch grips. Then form closure comes as an additional kinematic support. However, multi-finger grasping is outside the scope of this study mainly due to the fact that it is not required to demonstrate the performance of the proposed controller. Moreover, this study focused only the effect of stiffness variation on the controller. There are other types of sources such as variation of the moment created by tangential force due to more complex deformation of soft objects. This is an interesting future area to be studied. Since we limited our study to cylindrical objects to clearly demonstrate the effect of stiffness variation on the planar pinch grip controllers the ratio of the two tangential forces had a distribution with an average 1.0002 and standard

TABLE II
SUMMARY OF EXPERIMENTAL RESULTS. THE VALUES ARE GIVEN IN (AVERAGE, STANDARD DEVIATION^2) FORMAT.

	Tube-1				**Tube-2**			
	Proposed controller			**PID**	**Proposed controller**			**PID**
Criteria	$\delta = 0.2$	$\delta = 0.3$	$\delta = 0.4$		$\delta = 0.2$	$\delta = 0.3$	$\delta = 0.4$	
Probability of failure	$(0.28, 0.15^2)$	$(0.42, 0.2^2)$	$(0.48, 0.22^2)$	$(0.55, 0.22^2)$	$(0.29, 0.17^2)$	$(0.43, 0.2^2)$	$(0.49, 0.19^2)$	$(0.58, 0.23^2)$
Effort [rad/sec]	$(0.01, 0.03^2)$	$(0, 0.05^2)$	$(0, 0.06^2)$	$(0, 0.07^2)$	$(0.01, 0.04^2)$	$(0, 0.05^2)$	$(0, 0.06^2)$	$(0, 0.08^2)$
Grip force (F_n N)	$(6.02, 2.85^2)$	$(4.55, 1.63^2)$	$(4.18, 1.06^2)$	$(4.57, 1^2)$	$(6.67, 3.43^2)$	$(4.43, 1.28^2)$	$(4.21, 1.11^2)$	$(4.27, 0.99^2)$
Tube diameter [mm]	$(15.61, 2.72^2)$	$(17.58, 2.79^2)$	$(18.61, 3.37^2)$	$(17.93, 2.71^2)$	$(13.33, 2.96^2)$	$(14.7, 2.78^2)$	$(15.09, 2.2^2)$	$(15.01, 2.27^2)$

deviation 0.03 for the proposed controller (worse case scenario of $\delta = 0.04$), and that for the PID controller had an average 1.0008 and standard deviation 0.13. We can see from table II that these variations are negligible compared to the variability of the normal forces. However, we predict that variability of moment can be countered by introducing the same controller on roll of the object with a critical margin on the moment.

In the experiments and simulations, we took the moving window of 500 past samples of grip forces up to any given time to compute σ_{F_n} since it helps to account for the total range of interactions experienced by the gripper. A user may choose a different size of a moving window of forces to compute σ_{F_n}. However, this has to be done without posing the risk of making the probability of failure too sensitive to the recent behavior of the gripper itself.

The derivations in this paper considered only the stiffness variation of objects ignoring any effect due to damping. However, the fact that the proposed controller was stable in actual experiments show that the effect due to variation of damping in the rubber tubes is reasonably negligible. However, we would expect that any consideration of damping would inform the selection of the grip adaptation rate η because it determines how fast the grip adjustment should be made.

Future work for this controller includes automatic learning the critical force. One possible approach would be to use a prior assumption of a conservative critical force and learn an optimum value using break-away force prediction using our previous results [23] together with a suitable method to estimate the parameters of a friction model [32]. Our approach in [23] was based on the parameter identification of LuGre friction model [33] where the sliding contact between two surfaces is modeled as interactions of micro-elastic bristles. The approach requires the robotic hand to perform a short stroke haptic surface exploration to estimate the frictional properties of the finger-object contact. The break-away friction force is predicted at the state which results in a rapid increase in the bristles' displacements. A combination of the physical model based slip prediction approach in [23] with the proposed probabilistic approach for slip avoidance involves integrating slip detection to the controller. It will help to counter the uncertainty that comes from the friction coefficient itself though it is less crucial in the case of maintaining the grip at a given point as discussed in this paper. However, if the gripper were to lose contact momentarily, maintaining a safe grip at the new location may be jeopardized by an inaccurate estimate of the friction dynamics. On the other hand, slip can be used to estimate the friction coefficient.

REFERENCES

[1] N. E. Du Toit, & J. W. Burdick, "Robot motion planning in dynamic, uncertain environments", IEEE Transactions on Robotics, vol. 28, no. 1, pp. 101-115, 2012.

[2] J. Van Den Berg, P. Abbeel, & K. Goldberg, "LQG-MP: Optimized path planning for robots with motion uncertainty and imperfect state information", The International Journal of Robotics Research, vol. 30, no. 7, pp. 895-913, 2011.

[3] V. Lippiello, B. Siciliano, & L. Villani, "Multi-fingered grasp synthesis based on the object dynamic properties", Robotics and Autonomous Systems, vol. 61, no. 6, pp. 626-636, 2013.

[4] C. D. Takahashi, et al., "Impedance Control and Internal Model Formation when reaching in a Randomly Varying Dynamical Environment", *J. Neurophysiol*, vol. 86, pp. 1047 - 1051, 2001.

[5] T. Nanayakkara and R. Shadmehr, "Saccade Adaptation in Response to Altered Arm Dynamics", *Journal of Neurophysiology*, 2003, vol. 90, pp. 4016-4021.

[6] K. Hsiao, T. Lozano-Pérez, and L. P. Kaelbling, "Robust belief-based execution of manipulation programs," in *Eighth Intl. Workshop on the Algorithmic Foundations of Robotics*. 2008.

[7] R. J. Bickel and M. Tomizuka, "Disturbance Observer Based Hybrid Impedance Control"', *In procs. of the American Control Conference*, pp. 729 - 733, 1995.

[8] R. Kikuuwe and T. Yoshikawa, "Robot Perception of Environment Impedance", *In procs. of ICRA*, pp. 1661-1666, 2002.

[9] S. Lee and H. S. Lee, "'Intelligent Control of Manipulators Interfacing with an Uncertain Environment Based on Generalized Impedance", *In procs. of the IEEE Int. Symp. on Intelligent Control*, pp. 61-66, 1999.

[10] Z.-H. Jiang, "Impedance Control of Flexible Robot Arms with Parametric Uncertainties", *Journal of Intelligent and Robotic Systems*, vol. 42, pp. 113 - 133, 2005.

[11] T. Nanayakkara, K. Kiguchi, T. Murakami, K. Watanabe, K. Izumi, "Enhancing the Autonomy of Teleoperated Redundant Manipulators Through Fusion of Intelligent Control Modules," Journal of Robotics and Mechatronics, 14(3), pp.534-545, June, 2002.

[12] S. P. Chan and B. Yao, "Robust Impedance Control of Robot Manipulators", *Journal of Robotics and Automation*, vol. 6, no. 4, pp. 220 - 227, 1991.

[13] Y. Kishi, Z.W. Luo, F. Asano, and S. Hosoe, "Passive Impedance Control with Time-varying Impedance Centre", *In procs. of IEEE International Symposium on Computational Intelligence in Robotics and Automation*, vol. 3, pp. 1207-1212, 2003.

[14] A. Saxena, J. Driemeyer, J. Kearns, C. Osondu, and A. Y. Ng, "Learning to grasp novel objects using vision," in *In procs. of 10th International Symposium of Experimental Robotics (ISER)*. 2006.

[15] S. Hirai, T. Tsuboi, and T. Wada, "Robust grasping manipulation of deformable objects," in *In procs. of IEEE International Symposium on Assembly and Task Planning, 2001*. pp. 411–416, 2001.

[16] N. Mimura and Y. Funahashi, "Parameter identification of contact conditions by active force sensing," in *In procs. of IEEE International Conference on Robotics and Automation*. pp. 2645–2650, 1994.

[17] A. Petrovskaya, O. Khatib, S. Thrun, and A. Y. Ng, "Bayesian estimation for autonomous object manipulation based on tactile sensors," in *In procs. of IEEE International Conference on Robotics and Automation*. pp. 707–714, 2006.

[18] J. Laaksonen and V. Kyrki, "Probabilistic approach to sensor-based grasping," in *In procs. of ICRA 2011 Workshop on Manipulation Under Uncertainty*, 2011.

[19] P. R. Pagilla and M. Tomizuka, "Adaptive control of two robot arms carrying an unknown object," in *In procs. of IEEE International Conference on Robotics and Automation*, vol. 1. pp. 597–602, 1995.

[20] V. N. Christopoulos and P. Schrater, "Handling shape and contact location uncertainty in grasping two-dimensional planar objects," in *In procs. of IEEE/RSJ International Conference on Intelligent Robots and Systems*. pp. 1557–1563, 2007.
[21] F. Stulp, E. Theodorou, J. Buchli, and S. Schaal, "Learning to grasp under uncertainty," in *In procs. of IEEE International Conference on Robotics and Automation (ICRA)*. pp. 5703–5708, 2011.
[22] M. Takashi, S. Hiromitsu, and T. Kawai. "Control of grasping force by detecting stick/slip distribution at the curved surface of an elastic finger", *In procs. of IEEE International Conference on Robotics and Automation*, vol. 4, pp. 3895-3900, 2000.
[23] X. Song, H. Liu, K. Althoefer, T. Nanayakkara, and L. D. Seneviratne. "Efficient Break-Away Friction Ratio and Slip Prediction Based on Haptic Surface Exploration.", *IEEE trans. on Robotics*, vol. 30, no. 1, pp. 1-17, 2014.
[24] J. Nawid, and C. Sammut. "Slip prediction using Hidden Markov models: Multidimensional sensor data to symbolic temporal pattern learning." *In procs. of IEEE International Conference on Robotics and Automation (ICRA)* pp. 215-222, 2012.
[25] A. Jiang, J. Bimbo, S. Goulder, H. Liu, X. Song, P. Dasgupta, K. Althoefer, and T. Nanayakkara, "Adaptive grip control on an uncertain object." in *In procs. of IEEE/RSJ International Conference on Intelligent Robots and Systems (IROS)*. pp. 1161 - 1166, 2012.
[26] H. Liu, X. Song, J. Bimbo, L. Seneviratne, and K. Althoefer, 2012. October. Surface material recognition through haptic exploration using an intelligent contact sensing finger. In Intelligent Robots and Systems (IROS), 2012 IEEE/RSJ International Conference on (pp. 52-57). IEEE.
[27] H. Liu, K. C. Nguyen, V. Perdereau, J. Bimbo, J. Back, M. Godden, L. D. Seneviratne, and K. Althoefer, 2015. Finger contact sensing and the application in dexterous hand manipulation. Autonomous Robots, 39(1), pp.25-41.
[28] H. Liu, X. Song, J. Bimbo, K. Althoefer, and L. Senerivatne. "Intelligent Fingertip Sensing for Contact Information Identification." In Advances in Reconfigurable Mechanisms and Robots I, pp. 599-608. Springer London, 2012.
[29] A.W. Goodwin, P. Jenmalm, and R. S. Johansson. "Control of grip force when tilting objects: effect of curvature of grasped surfaces and applied tangential torque." *The Journal of neuroscience*, vol. 18, no. 24, pp. 10724-10734, 1998.
[30] R. Tinós and S. Yang, "Use of the q-Gaussian mutation in evolutionary algorithms"', *Soft Computing*, vol. 15, no. 8, pp. 1523-1549, 2011.
[31] Winitzki, Serge. "Uniform approximations for transcendental functions." *Computational Science and Its Applications — ICCSA 2003*, pp. 780-789. Springer Berlin Heidelberg, 2003.
[32] K. Worden; C.X. Wong; U. Parlitz; A. Hornstein; D. Engster; T. Tjahjowidodo; F. Al-Bender; D. D. Rizos; S. D. Fassois, "Identification of pre-sliding and sliding friction dynamics: Grey box and black-box models", *Mechanical Systems and Signal Processing*, vol.21, no. 1, pp. 514-534, 2007.
[33] K. J. Astrom, and C. Canudas-De-Wit. "Revisiting the LuGre friction model." *Control Systems*, vol. 28, no. 6, pp. 101 - 114, 2008.

Thrishantha Nanayakkara received the BSc and MSc degrees in electrical engineering from the University of Moratuwa (UM), Sri Lanka (1996), and Saga University (SU), Japan (1998), and PhD in robotics from SU (2001). He was a postdoctoral research fellow in the department of biomedical engineering, Johns Hopkins University, USA, 2001-2003; a senior lecturer in the faculty of engineering at the UM; a Radcliffe Fellow at Harvard University, USA (2008/09), and a research affiliate at MIT (2008/09), USA. He is currently a senior lecturer in the department of Informatics, King's College London. His research interests are in soft robotics, and robotic interaction with uncertain environments. He has published one textbook and more than 100 peer reviewed papers.

Allen Jiang is currently a Sr. Systems Engineer at Auris Surgical Robotics. He graduated with a BS in aerospace engineering in 2010 from the University of California, San Diego, and a PhD in robotics in 2014 from King's College London. His research interests include flexible manipulators, soft robotics, force sensing, and medical devices.

María del Rocío Armas Fernández received her M. Eng honors degree from King's College London, London, U.K in 2013. After her studies in Electronic Engineering she moved on to study International Relations at China Foreign Affairs University, Beijing, China and she has just recently received her LL.M in Diplomacy. She was involved in research on mechatronics in her third and final years of studies at King's College London and she has co-authored another paper based on metastable terrains.

Hongbin Liu is currently a lecturer (Assistant Professor) in the Department of Informatics, King's College London, UK, where he is leading the Robotic Contact Perception Lab. He received his B.S. degree in 2005 from the Northwestern Polytechnique University, Xi'an, China, and received MSc in 2006 and PhD degree in robotics in 2010 both from Kings College London, UK. He is a member of IEEE and Technical Committee Member for IEEE EMBS BioRobotics. His research interests include tactile/force perception, modelling and control of physical interaction, flexible and continuum robots, robotic grasping and manipulation.

Kaspar Althoefer (M'03) received the Dipl.-Ing. degree in electronic engineering from the University of Aachen, Aachen, Germany, and the Ph.D. degree in electronic engineering from King's College London, London, U.K. He is currently a Professor of Robotics and Intelligent Systems and Head of the Center for Robotics Research (CoRe), Department of Informatics, King's College London. He has been involved in research on mechatronics since 1992. He has authored or coauthored more than 180 refereed research papers related to mechatronics and robotics.

Joao Bimbo is currently a Postdoctoral researcher at the Advanced Robotics department at the Istituto Italiano di Tecnologia (IIT). He obtained an MSc in Electrical and Computer Engineering from the University of Coimbra in 2011 and a PhD in Robotics from King's College London in 2016. His research interests include robot grasping, tactile sensing and perception of objects' properties during manipulation.